24th COBEM - 2017

24th ABCM International Congress of Mechanical Engineering
December 3-8, 2017, Curitiba, PR, Brazil

COBEM-2017-5513
ANALYSIS OF COMPOSITE AND FUNCTIONALLY GRADED PLATES BEHAVIOUR CONCERNING TO BUCKLING

José S. Moita
Cristóvão M. Soares
IDMEC-IST, Universidade de Lisboa, Lisboa, Portugal.
jmoita50@gmail.com
cristovao.mota.soares@ tecnico.ulisboa.pt

José Herskovits
COOPE-UFRJ, Universidade Federal do Rio de Janeiro, Brasil.
jose@optimize.ufrj.br

Abstract. *In this work is presented the formulation for linear buckling and geometrically nonlinear analysis of laminated composite and functionally graded plates under in-plane loads and thermal loads, using an implemented finite element model based on a non-conforming triangular flat plate/shell element with 3 nodes, and 8 degrees of freedom per node, associated with a higher order shear deformation theory. The through the thickness variation of material properties, abruptly for laminated composite plates, or continuously for FGM plates, as well as of the temperature distribution, make this type of plates usually un-symmetric to the middle-surface. Thus, in general, for this type of plates, when they are subjected to mechanical in-plane load or thermal load, bending moments are develop together with the membrane forces, and consequently, the plate is deflected as soon as the load is applied. Due to this reason the occurrence of bifurcation-type buckling should be study, and the centre deflection of the plates is a good indicator to anticipate this occurrence.The solutions of some illustrative examples are performed, involving different lay-up, variation of volume fractions, temperature distributions, material combinations, etc., which have significant impacts on deflections of the plates. The results are presented, some of them are compared with numerical alternative models, and discussed.*

Keywords: *buckling, laminated composites, functionally graded materials, finite element.*

1. INTRODUCTION

In the last five decades a large number of researchers, including the present author, (Moita, *et al*.,1999, 2000, 2016), have done the buckling and geometrically nonlinear analyses of plate/shell structures using the finite element method, and considering different type of materials, like isotropic, composite and functionally graded materials.

In contrast with isotropic plates, in composite and functionally graded plates, the material properties vary through the thickness. Abruptly for laminated composite plates, and continuously for FGM plates. Furthermore, the variation of the thermal load in FGM plates is usually non-uniform through thickness. Thus, in general, when laminated composite and FGM plates are subjected to mechanical in-plane uniform load or thermal load, bending moments are develop together with the membrane forces, and consequently, the plate is deflected as soon as the load is applied. Therefore, in general, we can expect that the bifurcation-type buckling will not occur. With this in mind, Leissa (1986) did a theoretical study to find in what conditions the bifurcation-type buckling occurs for laminated composite plates. Some years later, Qatu and Leissa (1993) present a finite element study of four types of unsymmetrical laminates, including anti-symmetrical ones, considering various edge constraints and different in-plane applied load. In these works is found that in general, for the case of clamped edges, the support reacting moments produced by the four clamped edges neutralizes the generated moments and the plate can remain flat and thus buckling occurs. Also for the case of simply-supported plates is found that symmetric cross and angle-ply laminates, and antisymmetric angle-ply laminates buckling occurs.

From these conclusions, when we have functionally graded material (FGM) plates, that can be considered un-symmetric "composite" plates where the variation of material is made smooth and continuously, is expected for similar behaviour when they are acted by in-plane uniform mechanical load or thermal load. For the case of simply-supported isotropic plates under uniform temperature distribution, the thermal moments are equal to zero and only membrane forces are generated. Thus, the plate is still flat with no transverse deflection as temperature increases until reaches a critical value, and the plate suddenly buckles. For clamped FGM plates, by the same reason described above for laminated composite plates, is expected that buckling occurs. In conclusion, is expected that for mechanical in-plane load, buckling occurs for isotropic simply-supported or clamped plates, and for laminated composite and FGM clamped plates; for thermal load, buckling occur for isotropic, laminated composites and FGM clamped plates or for simply-supported isotropic or symmetric laminated composites plates under uniform temperature rise.

Research on buckling analysis of FGM structures has been done in the recent years. Among others, here we cite the following works: Javaheri and Eslami (2002) derived the equilibrium and stability equations for the rectangular functionally graded plates using the classical plate and high order shear deformation theories. Lanhe (2004) derived the equilibrium and stability equations of a

moderately thick rectangular plate made of functionally graded materials under thermal loads, based on the first order shear deformation theory. Na and Kim (2006) examined the effect of thermal loading and uniform pressure on the bending response of FGM plates. Wu *et al*., 2007 investigate the post-buckling response of FGM rectangular plate subjected to in-plane edge compressive loading and buckling of a FGM plate under uniform thermal loading. Zhao *et al*., 2009 analysed the mechanical and thermal buckling of functionally graded ceramic–metal plates using the first-order shear deformation plate theory. Nguyen *et al*., 2012 present a finite element model with node-based strain smoothing applied for static, free vibration and mechanical/thermal buckling. Thai and Choi (2012) present an efficient and simple refined theory for buckling analysis of functionally graded plates Natarajan *et al*., 2014 employed a cell-based smoothed finite element method with discrete shear gap technique to study the static bending, free vibration, and mechanical and thermal buckling behaviour of functionally graded material plates. Concerning buckling analysis of laminated composite plates subjected to mechanical in-plane loads, many works had been published. Thus we cite here some works used for comparison: Phan and Reddy (1985), Kozma and Ochoa (1986), Chakrabarti and Sheikh (2003). Considering thermal loads, published works can be found in the literature. Among others we cite the works of Thangaratnam *et al*.,1989 that used a semiloof finite element, Sun and Hsu (1990) presented closed form solution for simply supported plates with symmetric cross-ply laminations, and Chen *et al.*, 1991 using a quadrilateral finite element with eight nodes and the Mindlin theory.

In this paper is present the formulation for linear buckling and the nonlinear deformation analyses for laminated composite and functionally graded material plates. The solutions are obtained using a finite element model based on a non-conforming triangular flat plate/shell finite element with 3 nodes, and 8 degrees of freedom per node, and third order shear deformation theory. The solutions of some illustrative plate examples are performed, and the results are presented and discussed and compared with numerical alternative models.

2. SPECIFIC FORMULATION OF FGM MODEL

An FGM is made by mixing two distinct isotropic material phases, for example a ceramic and a metal. The material properties of an FGM plate structure is assumed to change continuously throughout the thickness, according to the volume fraction of the constituent materials. In this work is considered a model based on the power-law function to describe the volume fraction, combined with an approach based on virtual layers to estimate the effective material properties of the FGM at a point of the plate domain. The volume fraction of the ceramic and metal phases for each virtual layer is defined according to the power-law:

$$V_c^k = \left(0.5 + \frac{\bar{z}}{h}\right)^p \quad ; \quad V_m^k = 1.0 - V_c^k \tag{1}$$

Once the volume fractions have been defined, the material properties as Young's modulus E or thermal expansion coefficient α of each layer of an FGM can be determined by the rule of mixtures:

$$E_k = V_c^k\, E_c + V_m^k\, E_m \;\; ; \;\; \alpha_k = V_c^k\, \alpha_c + V_m^k\, \alpha_m \tag{2}$$

Since functionally graded plate structures are mainly used in high temperature environment and the mechanical properties of the constituent materials suffer significant changes with temperature increase, this temperature-dependency is considered in the present work. The temperature variation is assumed to occur in the thickness direction only, and can be obtained by solving a steady state heat transfer problem:

$$-\frac{d}{dz}\left[k(z)\frac{dT}{dz}\right] = 0 \tag{3}$$

where k(z) is the material thermal conductivity which is variable through the thickness direction and also temperature dependent. By imposing the boundary conditions of $\mathrm{T} = \mathrm{T_m}$ at $\mathrm{z} = -\mathrm{h}/2$ and $\mathrm{T} = \mathrm{T_c}$ at $\mathrm{z} = -\mathrm{h}/2$, the solution of this equation is obtained by means of a polynomial series as:

$$T(\bar{z}) = T_m + \frac{T_{cm}}{\xi}\left[\sum_{j=0}^{5} \frac{1}{j\;p+1}\left(-\frac{k_{cm}}{k_m}\right)^j \left(0.5 + \frac{z}{h}\right)^{jp+1}\right] \;;\; \xi = \sum_{j=0}^{5} \frac{1}{j\;p+1}\left(-\frac{k_{cm}}{k_m}\right)^j \tag{4}$$

and the properties of the constituent materials are obtained as follows

$$P = P_0\left(P_{-1}/T + 1 + P_1 T + P_2 T^2 + P_3 T^3\right) \tag{5}$$

where $T = T_0 + \Delta T$ and $\mathrm{T_0}$=300 K (ambient, or free stress temperature), and P_{-1}, P_1, P_2, P_3 are the coefficients of temperature (in Kelvin), and are unique to each constituent and ΔT is the temperature change.

3. NONLINEAR ANALYSIS THEORY.

3.1 Displacement field and strains

The present theory considers large displacements with small strains. The displacement field is based on the Reddy's third-order shear deformation theory:

$$u(x,y,z)=u_0(x,y)-z\,\theta_y(x,y)+z^3\,c_1\left[\theta_y(x,y)-\frac{\partial w_0}{\partial x}\right];\ v(x,y,z)=v_0(x,y)+z\,\theta_x(x,y)+z^3\,c_1\left[-\theta_x(x,y)-\frac{\partial w_0}{\partial y}\right];\ w(x,y,z)=w_0(x,y) \tag{6}$$

To the geometrically nonlinear behaviour, the Green's strain tensor is considered. Its components are conveniently represented in terms of the linear and non-linear parts of the strain tensor. The strain components associated with the displacement fields defined above are, for instance for x component:

$$\varepsilon_{xx}=\frac{\partial u_0}{\partial x}-z\,\frac{\partial\theta_y}{\partial x}+z^3c_1\left(\frac{\partial\theta_y}{\partial x}-\frac{\partial^2 w_0}{\partial x^2}\right);\ \gamma_{xy}=\frac{\partial u_0}{\partial y}+\frac{\partial v_0}{\partial x}+z\left(-\frac{\partial\theta_y}{\partial y}+\frac{\partial\theta_x}{\partial x}\right)+z^3c_1\left(\frac{\partial\theta_y}{\partial y}-\frac{\partial\theta_x}{\partial x}-2\frac{\partial^2 w_0}{\partial x\partial y}\right)$$

$$\gamma_{xz}=-\theta_y+\frac{\partial w_0}{\partial x}+z^2 3c_1\left(\theta_y-\frac{\partial w_0}{\partial x}\right);\ \varepsilon_{xx}^{NL}=\frac{1}{2}\left[\left(\frac{\partial u}{\partial x}\right)^2+\left(\frac{\partial v}{\partial x}\right)^2+\left(\frac{\partial w}{\partial x}\right)^2\right] \tag{7}$$

Considering thermal effect, the thermal strains for each virtual layer k, are then given by:

$$\varepsilon_k^{th}=\left\{\varepsilon_{xx}^{th}\quad\varepsilon_{yy}^{th}\quad 0\right\}_k^T=\left\{\alpha_k\,\Delta T_k\quad\alpha_k\,\Delta T_k\quad 0\right\}^T \tag{8}$$

3.2 Stress-strain relations and constitutive relations of FGM structures.

The stress-strain relations for each layer k, can be written as follows

$$\boldsymbol{\sigma}_k=\boldsymbol{Q}_k(\boldsymbol{\varepsilon}_k^{mec}-\boldsymbol{\varepsilon}_k^{th}) \tag{9}$$

where $\boldsymbol{\sigma}_k=\left\{\sigma_x\quad\sigma_y\quad\sigma_{xy}\quad\tau_{xz}\quad\tau_{yz}\right\}^T$ is the stress vector and $\boldsymbol{\varepsilon}_k=\left\{\varepsilon_x\quad\varepsilon_y\quad\gamma_{xy}\quad\gamma_{xz}\quad\gamma_{yz}\right\}^T$ is the strain vector, $\boldsymbol{\varepsilon}_k^{\mathrm{th}}$ and $\boldsymbol{\sigma}_k^{\mathrm{th}}$ are the thermal strain and stress vectors, and $\mathbf{Q}_k$ is the elasticity matrix. For each layer, linear elastic constitutive equation is given by:

$$\hat{\boldsymbol{\sigma}}_k=\hat{\boldsymbol{\sigma}}_{\mathrm{k}}^{\mathrm{mec}}-\hat{\boldsymbol{\sigma}}_{\mathrm{k}}^{\mathrm{th}}=\hat{\boldsymbol{D}}_{\mathrm{k}}\,(\boldsymbol{\varepsilon}_{\mathrm{k}}^{\mathrm{mec}}-\boldsymbol{\varepsilon}_{\mathrm{k}}^{\mathrm{th}})\ ;\ \hat{\boldsymbol{\sigma}}_k^{th}=\hat{\mathbf{D}}_k^{th}\,\boldsymbol{\varepsilon}_{\mathrm{k}}^{th}=\left\{\boldsymbol{N}^{th}\quad\boldsymbol{M}^{th}\quad\boldsymbol{M}^{*th}\right\}_k^T=\left[\mathbf{A}\quad\mathbf{B}\quad\mathbf{D}\right]_{\mathrm{k}}^{\mathrm{T}}\left\{\boldsymbol{\varepsilon}_{\mathrm{k}}^{th}\right\} \tag{10}$$

where $\hat{\boldsymbol{\sigma}}_{\mathrm{k}}$ are the resultant forces and moments, and $\hat{\mathbf{D}}_{\mathrm{k}}$ is the constitutive matrix.

4. FINITE ELEMENT FORMULATION. VIRTUAL WORK PRINCIPLE.

In the present work is used a non-conforming triangular plate/shell finite element model having three nodes and eight degrees of freedom per node: the displacements u_{0_i}, v_{0_i}, w_{0_i}, the slopes $(-\partial w_0/\partial y)_i$, $(\partial w_0/\partial x)_i$ and the rotations θ_{xi}, θ_{yi}, θ_{zi}. The rotation θ_{zi} is introduced to consider a fictitious stiffness coefficient $\mathrm{K}_{\theta\mathrm{Z}}$ to eliminate the problem of a singular stiffness matrix for general shape structures, Zienkiewicz (1977). The element local in-plane displacements u_0, v_0, as well as the rotations θ_x, θ_y are obtained in terms of the corresponding nodal variables through linear shape functions $\mathrm{L_i}$ given in terms of area co-ordinates, and the transverse displacement and slopes are expressed in terms of corresponding nodal variables through cubic shape functions ${}_{\mathrm{j}}\mathrm{N_i}$, Zienkiewicz (1977). The displacement field can be represented in matrix form as:

$$\boldsymbol{u}=\boldsymbol{Z}\,(\sum_{i=1}^{3}\boldsymbol{N}_i\,\boldsymbol{d}_i)=\boldsymbol{Z}\,\boldsymbol{N}\,\boldsymbol{a}\ \ ;\ \ \boldsymbol{d}=\sum_{i=1}^{3}\boldsymbol{N}_i\,\boldsymbol{d}_i=\mathbf{N}\,\mathbf{a}\ \ ;\ \ \boldsymbol{d}_{\mathrm{i}}=\left\{u_0\ \ v_0\ \ w_0\ \ -\frac{\partial w_0}{\partial y}\ \ \frac{\partial w_0}{\partial x}\ \ \theta_x\ \ \theta_y\ \ \theta_z\right\}_i \tag{11}$$

where $\mathbf{Z}$ is the appropriate matrix containing powers of $\mathbf{Z}_{\mathrm{k}}$, $\mathbf{a}$ is the element displacement vector, and $\mathbf{d}_i$ is the nodal displacement vector.The membrane, bending and shear strains, as well the higher order bending and shear strains can be represented by:

$$\varepsilon_m=\boldsymbol{B}^m\,\boldsymbol{a}\ ;\ \varepsilon_b=\boldsymbol{B}^b\,\boldsymbol{a}\ ;\ \varepsilon_s=\boldsymbol{B}^s\,\boldsymbol{a}\ ;\ \varepsilon_b^*=\boldsymbol{B}^{*\mathrm{b}}\,\boldsymbol{a}\ ;\ \varepsilon_s^*=\boldsymbol{B}^{*\mathrm{s}}\,\boldsymbol{a} \tag{12}$$

where $\mathbf{B}^m$, $\mathbf{B}^b$, $\mathbf{B}^{*b}$, $\mathbf{B}^s$, $\mathbf{B}^{*\mathrm{s}}$, are components of the strain-displacement matrix $\mathbf{B}$, given in Moita *et al*., 2011.

The governing equations for nonlinear analysis are obtained from the Principle of Virtual Work in conjugation with an updated Lagrangian formulation. A reference configuration is associated with time *t* and the actualized configuration is associated with the

current time $t' = t + \Delta t$. Taking the Virtual Work Principle, doing the incremental decomposition of the stress and strain tensors, we obtain in an incremental form for the thermo-mechanical nonlinear analysis:

$$\sum_{k=1}^{N} \left\{ \int_{{}^{t}A^{e}} \int_{h_{k-1}}^{h_k} \left[\delta({}_{t}\boldsymbol{\varepsilon}_{k}^{mec} - \boldsymbol{\varepsilon}_{k}^{th})\, \mathbf{Q}_k\, ({}_{t}\boldsymbol{\varepsilon}_{k}^{mec} - \boldsymbol{\varepsilon}_{k}^{th})\, dz\, {}^{t}dA^{e} + \delta\, {}_{t}\boldsymbol{\varepsilon}_{k}^{NL}\, ({}^{t}\boldsymbol{\sigma}_{k}^{mec} - {}^{t}\boldsymbol{\sigma}_{k}^{th})\, dz\, {}^{t}dA^{e} + \delta({}_{t}\boldsymbol{\varepsilon}_{k}^{mec} - \boldsymbol{\varepsilon}_{k}^{th}\, ({}^{t}\boldsymbol{\sigma}_{k}^{mec} - \boldsymbol{\sigma}_{k}^{th})\, dz\, {}^{t}dA^{e} \right] \right\} = {}^{t+\Delta t}_{t}\Re^{e} \qquad (13)$$

Integrating through the thickness in each layer k, summing over the total thickness, doing the mathematical development and eliminating the virtual displacement vector $\delta \mathbf{a}^{e}$, comes:

$$\int_{{}^{t}A^{e}} \left(\boldsymbol{B}^{T} \hat{\boldsymbol{D}}\, \boldsymbol{B} + \boldsymbol{G}^{T} (\hat{\sigma}^{mec} - \hat{\sigma}^{th})\, \boldsymbol{G}^{t} \right) {}^{t}dA^{e}\, \Delta \boldsymbol{a}^{e} = \boldsymbol{F}_{c} + \int_{{}^{t}A^{e}} \left(\boldsymbol{N}^{T} \boldsymbol{f} + \boldsymbol{N}^{T} \boldsymbol{t} + \boldsymbol{B}^{T} \tilde{\sigma}^{th} - \boldsymbol{B}^{T} ({}^{t}\tilde{\sigma}^{mec} - \tilde{\sigma}^{th}) \right) {}^{t}dA^{e} \qquad (14)$$

where the linear, geometric, and initial thermal stress stiffness matrices, external mechanical forces (including distributed and concentrated transverse loads **f** and $\mathbf{F}_c$, in-plane xy load **t**) and internal forces vector are given by:

$$\mathbf{K}_{L}^{e} = \int_{{}^{t}A^{e}} \boldsymbol{B}^{T} \hat{\boldsymbol{D}}\, \boldsymbol{B}\, dA^{e}\ ;\ \boldsymbol{K}_{G}^{e} = \int_{{}^{t}A^{e}} \boldsymbol{G}^{T} \hat{\sigma}^{mec}\, \boldsymbol{G}\, dA^{e}\ ;\ \boldsymbol{K}_{0}^{e} = \int_{{}^{t}A^{e}} \boldsymbol{G}^{T} (-\hat{\sigma}^{th})\, \boldsymbol{G}\, dA^{e}\ ;\ F^{e}{}_{int} = \int_{{}^{t}A^{e}} \boldsymbol{B}^{T} \left({}^{t}\tilde{\sigma}^{mec} - {}^{t}\tilde{\sigma}^{th} \right) {}^{t}dA^{e} \qquad (15)$$

$$\boldsymbol{F}^{e\,mec} = \int_{A^{e}} \boldsymbol{N}^{T}\, \boldsymbol{f}\, dA^{e} + \int_{S^{e}} \boldsymbol{N}^{T}\, \boldsymbol{t}\, dS^{e} + \boldsymbol{F}_{c}\ ;\ \mathbf{F}^{e\,th} = \int_{A^{e}} \mathbf{B}^{T} \tilde{\sigma}^{th}\, dA^{e} = \left\{ \boldsymbol{B}^{m\,T} \quad \boldsymbol{B}^{b\,T} \quad \boldsymbol{B}^{*b\,T} \right\} \left\{ \begin{matrix} \boldsymbol{N}^{th} \\ \boldsymbol{M}^{th} \\ \boldsymbol{M}^{*th} \end{matrix} \right\} \qquad (16)$$

$$\tilde{\sigma}^{mec} = \left\{ \begin{array}{c|c|c} N_{xx}^{m} & M_{xx}^{b} & M_{xx}^{*b} \\ N_{yy}^{m} & M_{yy}^{b} & M_{yy}^{*b} \\ N_{xy}^{m} & M_{xy}^{b} & M_{xy}^{*b} \end{array} \right\};\ \hat{\sigma}^{mec} = \begin{bmatrix} N_{xx} & N_{xy} & 0 & 0 & 0 & 0 \\ N_{xy} & N_{yy} & 0 & 0 & 0 & 0 \\ 0 & 0 & N_{xx} & N_{xy} & 0 & 0 \\ 0 & 0 & N_{xy} & N_{yy} & 0 & 0 \\ 0 & 0 & 0 & 0 & N_{xx} & N_{xy} \\ 0 & 0 & 0 & 0 & N_{xy} & N_{yy} \end{bmatrix};\ \hat{\sigma}^{th} = \begin{bmatrix} N_{xx}^{th} & 0 & 0 & 0 & 0 & 0 \\ 0 & N_{yy}^{th} & 0 & 0 & 0 & 0 \\ 0 & 0 & N_{xx}^{th} & 0 & 0 & 0 \\ 0 & 0 & 0 & N_{yy}^{th} & 0 & 0 \\ 0 & 0 & 0 & 0 & N_{xx}^{th} & 0 \\ 0 & 0 & 0 & 0 & 0 & N_{yy}^{th} \end{bmatrix} \qquad (17)$$

Summing the contribution of each layer, adding the contributions of all the elements in the domain, and doing local - global transformations to solve general structures, yields:

$${}^{t+\Delta t}_{t+\Delta t}(\mathbf{K}_{L} + \mathbf{K}_{G} + \boldsymbol{K}_{0})^{i-1} (\Delta \boldsymbol{q})^{i} = {}^{t+\Delta t}\boldsymbol{F}^{mec} + \boldsymbol{F}^{th} - {}^{t+\Delta t}_{t+\Delta t}(\boldsymbol{F}_{int})^{i-1} \qquad (18)$$

For linear mechanical/thermal buckling analysis, we make use of only one load increment. The instability takes place when the determinant of the tangential matrix is zero. It occurs for a certain value of geometric/initial stress stiffness matrix defined by ${}^{cr}\mathbf{K}_{L} = \lambda_{cr}\, \mathbf{K}_{G}$ or ${}^{cr}\mathbf{K} = \lambda_{cr} \mathbf{K}_{0}$. Thus, linear elastic buckling standard eigenvalue problem is then given by $(\mathbf{K}_{L} + \lambda_{cr} \mathbf{K}_{G})\, \boldsymbol{q} = 0$ or $(\boldsymbol{K}_{L} + \lambda_{cr} \boldsymbol{K}_{0})\, \boldsymbol{q} = 0$ and the critical load is ${}^{cr}\boldsymbol{F}^{mec} = \lambda_{cr}\, \boldsymbol{F}_{0}^{mec}$ or ${}^{cr}\boldsymbol{F}^{th} = \lambda_{cr}\, \boldsymbol{F}_{0}^{th}$ or ${}^{cr}\Delta T = \lambda_{cr}\, \Delta T$, where λ_{cr} represents the buckling parameter. The solution of linear buckling problem consists firstly of the solution of the static load-displacement problem, the initial stress matrix resulting from the solution of static problem.

5. APPLICATIONS

5.1 – Mechanical buckling of Simply-Supported and Clamped Laminated Composite Plates

The linear buckling analysis of square (axa) laminated plates with all edges simply-supported (SSSS) or clamped (CCCC) are considered. The material properties of the individual layers are given by: a) $E_1/E_2=40$, $G_{12}=G_{13}=0.6\ E_2$, $G_{23}=0.5\ E_2$, $\nu_{12} = \nu_{13} = 0.25$ and a/h=10. Simply-supported plates with symmetric cross-ply [0º/90º/90º/0º] (SYCP) and antisymmetric cross-ply [0º/90º/0º/90º] (ASCP) laminations, symmetric angle-ply [45º/-45º/-45º/45º] (SYAP, and un-symmetric lamination [0º/15º/30º/45º] (UNSYM); b) $E_1/E_2=25$, $G_{12}=G_{13}=0.5\ E_2$, $G_{23}=0.2\ E_2$, $\nu_{12} = \nu_{13} = 0.25$ and a/h=10 for simply-supported plate with antisymmetric angle-ply lamination [45º/-45º/45º/-45º] (ASAP). The boundary conditions considered are given in Table 1. The obtained normalized critical loads $\bar{N}_{cr} = N_{cr}\, (a^{2} / E_{2} h^{3})$ are given in Table 2 for comparison and validation of the present model. It is observe that the present model (P) agree very well with alternative results obtained by Kozma and Ochoa (1986), [1], and Chakrabarti and Sheikh (2003), [2]. In the following tables are also given the centre displacement w_c related to an initial load $p_{xx}^{0} = 1 MPa$, and where w_c= ~ 0 means centre displacement $0.0 < |w_c\, (mm)| < 1.0\, x\, 10^{-15}$. In Table 3 are presented the results obtained with the present model for clamped plates, considering the material properties of case a) and the result obtained by Phan and Reddy (1985), [3].

Table 1. Boundary conditions

Boundary	Side y=0	Side y=a	Side x=0	Side x=a
SSSS	$w=0,\theta_y=0$	$v=0,w=0,\theta_y=0$	$w=0,\ \theta_x=0$	$u=0,w=0,\theta_x=0$
CCCC	$w=0,\theta_x,\theta_y=0$	$v=0,w=0,\theta_x=0,\theta_y=0$	$w=0,\ \theta_x=0,\theta_y=0$	$u=0,w=0,\theta_x=0,\theta_y=0$

Table 2. Normalized critical axial load $\overline{N}_{cr}$ of simply-supported laminated composite plates

	Symmetric		Antisymmetric		Un-symmetric
	a) SYCP	a) SYAP	a) ASCP	b) ASAP	[0º/15º/30º/45º]
$\overline{N}_{cr}$	23.30 [1]	24.99 [2]	22.58 [1]	19.63 [1]	-
	23.30 (P)	27.24 (P)	22.67 (P)	19.66 (P)	14.53 (P)
w_c(mm)	0.0	0.0	$-6.03\text{x}10^{-4}$	~ 0	$-2.56\text{x}10^{-3}$

Table 3. Normalized critical axial load $\overline{N}_{cr}$ of clamped laminated composite plates

	Symmetric		Antisymmetric		Un-symmetric
	a) SYCP	a) SYAP	a) ASCP	a) ASAP	a)[0º/15º/30º/45º]
$\overline{N}_{cr}$	-	31.08 [3]	-	-	-
	41.26 (P)	30.20 (P)	37.05 (P)	34.88 (P)	24.37 (P)
w_c(mm)	0.0	0.0	~0	~0	$2.72\text{x}10^{-5}$

5.2 Mechanical Buckling of Simply-Supported and Clamped FGM plates

The linear buckling analysis of a square (axa) P-FGM plate (Al/Al_2O_3) with all edges simply-supported made of a mixture of alumina and aluminium is considered. The material properties for the alumina and aluminium are E_c=380.0 GPa, $\nu_c = 0.25$, E_m = 70.0 GPa, $\nu_m = 0.25$. The side length takes the values a=1.0 m, a=0.2 m and a=0.1 m. The thickness of the plate is h=0.01 m. The FGM plates are under uniaxial compression and the power law index-p takes different values. Considering the buckling parameter $\overline{N}_{cr} = N_{cr}(a^2 / E_m h^3)$, the results obtained using the present model are shown in Table 4 and compared with the results of Thai and Choi (2012).

Table 4. Buckling parameter of simply-supported Al/Al_2O_3 FGM plates under uniaxial compression

a/h	Source	Power Law Index				
		Ceramic	0.5	1.0	2.0	5.0
10.	Thai & Choi, (2012)	18.5785	12.1229	9.3391	7.2631	6.0531
	PM	18.5616	12.2431	9.5007	7.4512	6.1498
20.	Thai & Choi (2012)	19.3528	12.5668	9.6675	7.5371	6.3448
	PM	19.3454	12.7119	9.8633	7.7672	6.4993
	w_c x 10^{-3} (mm)	0.0	4.75	9.47	15.6	18.8
10.	Thai & Choi (2012)	19.6145	12.7158	9.7775	7.6293	6.4507
	PM	19.6874	12.9118	10.0232	7.9021	6.3353

The buckling analysis of the previous square (axa) P-FGM plate, now with all edges movable and clamped, is investigated. The FGM plates are under uniaxial compression and the power law index takes different values. The critical buckling parameter is defined as $\lambda_{cr} = N_{cr}^b b^2 / E_c h^3$. Table 5 shows the critical buckling parameters for the FGM plates under mechanical loads for the cases of side-to-thickness ratios of a/h=100, 40. From the results obtained using the present model (PM), is observed a very good agreement with those obtained by Wu et al., 2007. Also the influence of the power-law p-index, observed in the Table 5 are according with what would be predictable, i.e., the buckling strength of FGM plates are more than fully metal plate made of aluminium and less than that of fully ceramic plate made of alumina. It can also be observed that the buckling strength decrease with increase of p-index.

Table 5. Buckling parameter of clamped Al/Al_2O_3 FGM plates under uniaxial compression.

a/h	Source	Power law index				
		Ceramic	1.0	2.0	5.0	Metal
100	Wu et al.,2007	9.158	4.616	3.579	3.034	-
	PM	9.426	4.718	3.643	3.078	1.744
40.	Wu et al., 2007	9.062	4.582	3.570	2.999	1.678
	PM	9.158	4.591	3.572	2.995	1.689

The buckling analysis of a square (axa) P-FGM plates with all edges movable and clamped, made of a mixture of zirconia and aluminium (Al/ZrO2), is also considered. The material properties for the zirconia, alumina and aluminium are E_c=151.0x10^9

N/m^2, $\nu_c = 0.3$, E_m = 70.0x10^9 N/m^2, $\nu_m = 0.3$. The FGM plates are under uniaxial compression and the power law index-p takes different values. The critical buckling parameter is defined as $\lambda_{cr} = N_{xx}\, a^2 / D_0$, where $D_0 = E_m\, h^3 / 12(1-\nu^2)$. The results are shown in Table 6. From this table is observed an excellent agreement between the results obtained using the present model (PM) with those obtained using MITC4 model, and are in between of those obtained by DSG, Nguyen *et al.*, 2012, [4], and Kp-Ritz models, Zhao *et al*., 2009, [5]. The first four models use a first-order shear deformation while the present model use a third-order shear deformation theory and 20x20 mesh (800 triangular elements).

Table 6. Buckling parameter of clamped square Al/ZrO2 FGM plates under uniaxial compression, with a=0.2 m, h=0.01 m

Model	Ceramic	p=0.2	p=0.5	p=1.0	p=2.0	p=5.0
DSG3 [4]	207.447	183.827	162.619	145.294	132.871	122.819
NS-DSG3 [4]	203.974	180.754	159.902	142.866	130.648	120.755
MITC4 [4]	203.497	180.331	159.529	142.533	130.342	120.471
Kp-Ritz [5]	195.913	173.588	153.559	137.203	125.498	116.055
PM	203.382	180.791	159.803	142.644	130.026	119.934
w_c	0.0	~ 0	~ 0	~ 0	~ 0	~ 0

5.3 Thermal buckling of Simply-Supported and Clamped Laminated Composite Plates.

The buckling analysis of square (axa) laminated plates with all edges fixed (SSSS) or clamped (CCCC) are considered. The material properties are E_1=200.0 GPa, E_2=10. GPa, $G_{12}=G_{13}=G_{23}$=5.0 GPa, ν_{12} = 0.25, $\alpha_1 = 1.0x10^{-6}/^0C$, $\alpha_2 = 2.0x10^{-6}/^0C$. The thermal buckling is computed for uniform temperature rise through the thickness with a/h=100, and linear temperature distribution with a/h=40. Three types of lamination are considered: symmetric laminations [0º/90º/90º/0º], [45º/-45º/-45º/45º], antisymmetric laminations [0º/90º/0º/90º], [45º/-45º/45º/-45º] and un-symmetric lamination [0º/30º/45º/60º]. Solving the eigenvalue problem the critical temperatures obtained are given in Tables 7-8, where is also given the centre displacement w_c (mm) related with an initial $\Delta T = 10^o C$. For the case of antisymmetric angle-ply lamination are used (5) layers to compare the present results with those of Thangaratnam *et al*., 1989, [6], which results are taken from the graphics (*). Two conclusions arise from the Tables 7-8:

Table 7. Critical temperature ΔT_{cr} of laminated composite plates under uniform temperature rise (a/h=100).

		Symmetric		Antisymmetric		Un-symmetric
		cross-ply	angle-ply	cross-ply	angle-ply	
SSSS	PM	83.74	110.42 (5)	82.01	114.44	68.36
	[6]	82.51	* 109. (5)	-	* 111.	-
w_c (mm)	PM	~ 0	~ 0	~ 0	~ 0	-1.28x10^{-2}
CCCC	PM	278.60	219.39 (5)	266.74	214.60	116.42
	[6]	* 270.	* 223. (5)	-	* 204.	-
w_c (mm)	PM	0.0	0.0	~ 0	~ 0	~ 0

Table 8. Critical temperature ΔT_{cr} of laminated composite plates under linear temperature distribution (a/h=40).

		Symmetric		Antisymmetric		Un-symmetric
		cross-ply	angle-ply	cross-ply	angle-ply	
SSSS	PM	1092.04	1329.91	1069.31	1458.04	915.89
w_c (mm)		4.24x10^{-2}	2.89x10^{-2}	4.26x10^{-2}	2.77x10^{-2}	4.03x10^{-2}
CCCC	PM	3976.28	2962.70	3638.84	2861.73	1583.37
w_c (mm)	PM	~ 0	~ 0	~ 0	~ 0	~ 0

a) the results obtained with the present model are in good agreement with the those of Thangaratnam *et al*.,1989.
b) for all situations of symmetric temperature distribution (uniform), unless for the case of un-symmetric lamination and SSSS plate, the centre displacement is w_c=0 or w_c ~ 0, meaning that bifurcation-type buckling occurs.
c) for all situations of un-symmetric temperature distribution (linear), and SSSS plate, the centre displacement is $w_c \neq 0$, what means that a bifurcation-type occurs. For CCCC boundaries the centre displacement is w_c ~ 0, and thus bifurcation-type not occurs.

5.4 Thermal buckling of Simply-Supported and Clamped FGM Plates.

The thermal buckling behaviour of a simply supported FGM (Al/Al_2O_3) square plate is studied next. The top surface is ceramic rich and the bottom surface is metal rich. A nonlinear temperature distribution across the plate thickness is considered. The critical buckling temperature difference ΔT_{cr} for different p-index are given in Table 9. The obtained results are compared with those obtained by Javaheri and Eslami (2002), [7], and Natarajan *et al*., 2014, [8], and a good agreement is observed. Is also studied the thermal buckling of the same FGM square plate considering uniform temperature rise (UTD) with all sides simply supported (SSSS). The results are presented in Table 10. It can be observed a very good agreement between the results obtained with the present model and those given by Javaheri and Eslami (2002) using the higher order model.

Table 9. Critical buckling temperature for simply-supported FGM square plates with different a/h, considering nonlinear temperature rise through the thickness: $\Delta T_{cr} = \lambda_{cr}(T_c - T_m)$

SSSS		Power law index						
a/h	Source	Ceramic	p=0.5	p=1.0	p=2.0	p=5.0	p=10.0	Metal
	CPT [7]	3409.8	-	2055.0	-	1553.3	1519.5	-
10.	HSDT[7]	3224.9	-	1960.0	-	1450.7	1408.1	-
	[8]	3261.2	-	1979.3	-	1483.5	1442.6	-
	PM	3234.2	2440.8	1970.6	1610.0	1450.8	1402.1	1040.9
	CPT [7]	844.9	-	503.9	-	380.2	372.2	-
20.	HSDT [7]	833.0	-	497.9	-	373.2	364.8	-
	PM	841.5	631.2	510.3	418.1	380.9	370.2	270.2
	w_c x 10^{-2}(mm)	1.41	1.43	1.40	1.38	1.69	2.21	4.39

Table 10. Critical buckling temperature $\Delta T_{cr} = \lambda_{cr}\, T_u$ for FGM simply-supported square plates with a/h=10, considering uniform temperature rise through the thickness: $T_u=T_c=T_m$

SSSS	Power law index						
a/h=10.	ceramic	p=0.5	p=1.0	p=2.0	p=5.0	p=10.	Metal
CPT [7]	1709.9	-	794.3	-	726.5	746.9	-
HSDT [7]	1617.4	-	757.8	-	678.9	692.5	-
PM	1617.2	924.1	756.8	666.7	673.9	685.0	520.3
w_c x 10^{-3} (mm)	~ 0	-5.6	-7.4	-8.3	-7.0	-5.2	~ 0

A square FGM plate (Al/Al_2O_3) with all sides clamped, made of a mixture of alumina and aluminium is considered. The thermal buckling is obtained for nonlinear temperature distribution through the thickness, for plate with a/h=10. The critical buckling temperature difference ΔT_{cr} for different p-index are given in Table 11. Also the thermal buckling is obtained for uniform temperature rise through the thickness. Two side to thickness ratios a/h=10 and a/h=100 are considered. The results are presented in Table 12, and compared with those taken from the graphics (*) of Nguyen *et al.*, 2012, [4]. A good agreement is observed.

Table 11. Critical buckling temperature ΔT_{cr} for FGM clamped square plates considering nonlinear temperature rise through the thickness: $\Delta T_{cr} = \lambda_{cr}(T_c - T_m)$.

CCC	Source	Power law index						
a/h		Ceramic	p=0.5	p=1.0	p=2.0	p=5.0	p=10.0	Metal
20.0	PM	2176.1	1641.20	1325.5	1084.0	980.4	948.1	700.2
	w_c	~ 0	~ 0	~ 0	~ 0	~ 0	~ 0	~ 0

Table 12. Critical buckling temperature $\Delta T_{cr} = \lambda_{cr}\, T_u$ for FGM clamped square plates considering uniform temperature rise through the thickness: $T_u=T_c=T_m$

CCC	Source	Power law index						
a/h		Ceramic	p=0.5	p=1.0	p=2.0	p=5.0	p=10.0	Metal
10.0	Ref [4]*	3860.0			1610.0			-
	PM	3887.0	2242.7	1840.3	1609.7	1583.7	1593.06	1250.6
100.0	Ref [4]	46.3	26.5	21.5	19.0	19.50	20.00	-
	PM	45.80	26.14	21.33	18.85	19.30	19.80	19.80
	w_c	0.0	~ 0	~ 0	~ 0	~ 0	~ 0	0.0

Table 13. Critical buckling temperature $\Delta T_{cr} = \lambda_{cr}\, T_u$ for FGM clamped square plates considering nonlinear temperature rise through the thickness: $T_u=T_c=T_m$

CCCC		Power law index		
a/h	Source	p=0.3	p=1.0	p=5.0
100.0	Na & Kim (2006)	34.17	30.56	28.21
	PM	34.42	30.61	29.09
50.0	Na & Kim (2006)	135.93	121.53	112.15
	PM	134.05	119.28	113.14

Next, a clamped square FGM plate made of a mixture of alumina and nickel is considered. The material properties for the alumina and nickel are: E_c=393.0 GPa, $\nu_c = 0.25$, $\alpha_c = 8.8x10^{-6}/^0C$, E_m = 199.5 GPa, $\nu_m = 0.3$, $\alpha_m = 13.3\,x10^{-6}/^0C$. Thermal buckling is analysed for uniform temperature rise through the thickness The results for a/h=100 and a/h=50 are presented in Table 13,

and compared with those from Na and Kim (2006). From Table 13, we observe an excellent agreement between the present results with those given from the above mentioned authors.

5.5 Nonlinear analyisis

The correct analysis of plates subjected to in-plane mechanical load or thermal load for the cases where the bifurcation phenomena do not occur is a geometrically nonlinear analysis. First, we summarize in Tables 14-15 the occurrence of linear buckling for the cases considered above. Next we perform the geometrically nonlinear analysis to obtain the correct response of these types of plates, expecting the confirmation of the previous study.

Table 14. Linear buckling occurrence for laminated composite plates

		Laminated composite plates			
Bound.	Load	Lay-up			
		SYMM	ASCP	ASAP	USYM
SSSS	Mech	Yes	No	Yes	No
	UTD	Yes	Yes	Yes	No
	LTD	No	No	No	No
CCCC	Mech	Yes	Yes	Yes	?
	UTD	Yes	Yes	Yes	Yes
	LTD	Yes	Yes	Yes	Yes

Table 15. Linear buckling occurrence for FGM plates

	Functionally graded plates					
Boundary	In-plane load		Temperature distribution			
			Uniform		non-uniform	
	CER/MET	FGM	CER/MET	FGM	CER/MET	FGM
SSSS	Yes	No	Yes	No	No	No
CCCC	Yes	Yes	Yes	Yes	Yes	Yes

5.6. Laminated Composite Plates under Mechanical Load

Square (axa) laminated plates with all edges simply-supported (SSSS) or clamped (CCCC) are considered. The material properties are E_1=229 GPa, E_2=13.5 GPa, G_{12}=G_{13}=G_{23}=5.25 GPa, ν_{12} = 0.3151**.** The side length is a=0.225 m and the thickness of the plate is h=0.01m. These plates are subjected to an incremental in-plane compressive applied load. The laminations analysed are: symmetric lamination [0º/90º/90º/0º] and antisymmetric laminations [0º/90º/0º/90º], [90º/0º/90º/0º] and un-symmetric lamination [0º/15º/30º/45º]. In Figures 1-3, the load-displacement paths of centre point of SSSS and CCCC plates are shown. For this and all applications, to trace the load-displacement paths, for the cases of Yes of Tables 14 and 15, an imperfection initial plate is considered, which consists, in general, in an initial centre displacement $w_c^0 = h/100$. We observe from Figure 1 that the SSSS symmetric laminated plate has a buckling load of about $\sigma_{cr} = 410.0\,MPa$ which agrees with the obtained eigenvalue $\sigma_{cr} = 416.080 MPa$. Is also observed that the SSSS anti-symmetric cross-ply laminated, plates don't reach suddenly a high defection, which means that no buckling load occurs. From Figure 2, as the plates have all edges clamped, we observe that in all of them buckling occurs, and the buckling loads are close to the obtained eigenvalues. All of these results confirm Table 14.

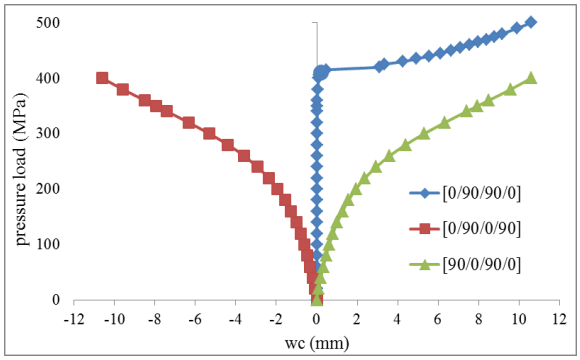

Figure 1. Load-displacement paths of SSSS composite plates.

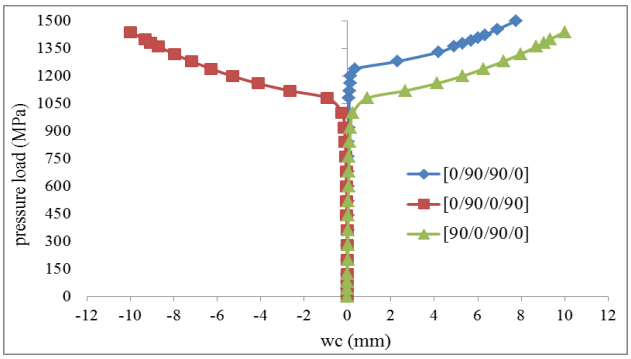

Figure 2. Load-displacement paths of CCCC composite plates

Next the un-symmetric laminated plates are investigated. The results are shown in Figure 3. From this Figure is observed that for SSSS un-symmetric plate no buckling occur. For the clamped plate, although the correct response is given by the geometric nonlinear analysis, the linear buckling analysis is acceptable.

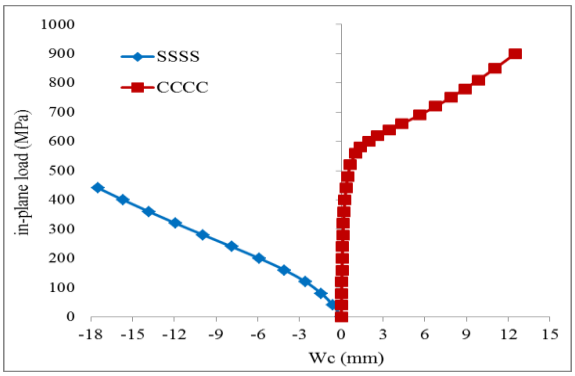

Figure 3. Load-displacement paths of SSSS and CCCC un-symmetric laminated composite plates

5.7 FGM Plates under Mechanical Load

A simply-supported square (axa) P-FGM plate, made of a mixture of zirconia and aluminium, is considered. The material properties for the alumina and aluminium are E_c=380. GPa, $\nu_c = 0.3$, E_m = GPa, $\nu_m = 0.3$. The side length is a=0.2 m and the thickness is h=0.01 m. The FGM plates are under uniaxial compression and the power law index-p takes different values. In Figure 4 is shown the load-displacement paths for applied uniaxial compression for isotropic and FGM plates (p=0, p=1 and p=5). To the normalized eigenvalues obtained previously, see Table 4, corresponds the following critical stresses: p=0 - $\sigma_{cr} = 3385445 MPa$; p=1 - $\sigma_{cr} = 1726077 MPa$; p=5 - $\sigma_{cr} = 1137377 MPa$. From Figure 4 we observe that the critical stress for isotropic pure ceramic plate compares very well with the corresponding obtained eigenvalue. On other hand the response of the two FGM plates (p=1.0 and p=5.0) confirms Table 13, i. e., linear buckling does not occur. Considering the same FGM plate, now with all edges clamped and a/h=100, the load-displacement paths obtained are given in Figure 5. Again we observe an agreement with Table 10 and with the buckling loads obtained by solving the eigenvalue problem: p=0, $\sigma_{cr} = 3582 MPa$ and p=1.0, $\sigma_{cr} = 1793 MPa$.

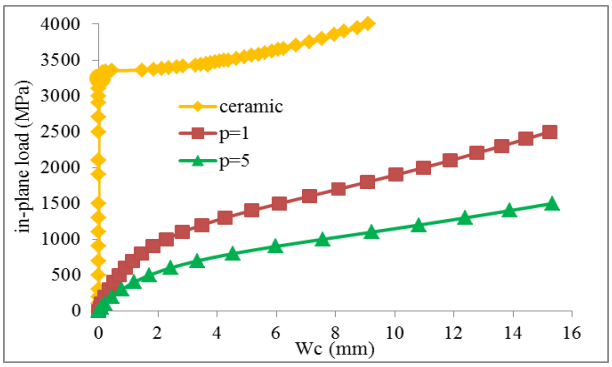

Figure 4. Load-displacement path for simply-supported FGM plate

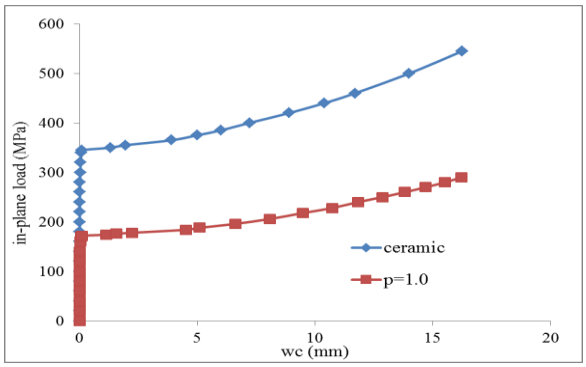

Figure 5. Load-displacement path for clamped FGM plate.

5.8 Simply-supported FGM Plates under Thermal Load.

The nonlinear deformation behaviour of a simply supported (all sides fixed) square FGM plate made of alumina/aluminium with a/h=0.1, investigated. The material properties of the constituents are independent of the temperature:

$E_c = 380 GPa$, $\nu_c = 0.3$, $\alpha_c = 7.4 x10^{-6}/^0C$, $K_c = 10.4 W/mK$, $E_m = 70 GPa$, $\nu_m = 0.3$, $K_m = 204 W/mK$ $\alpha_m = 23.0 x10^{-6}/^0C$.

Figure 6 shows the thermal load-displacement path for an isotropic plate under uniform temperature rise is considered and is observed the bifurcation phenomena. Also is observed that the bifurcation point is approximately at T=1550 K, while the eigenvalue is T=1617 K. In Figure 7 are shown the thermal load-displacement paths for isotropic plate and FGM plate with index p=1 for the case of nonlinear temperature distribution. The eigenvalues previously obtained are ΔT=3375 and ΔT=2198 respectively. From the Figures 7-8, is also observed that the responses of the plates confirm Table 15.

6. CONCLUSIONS

The bifurcation-type buckling of laminated composite and functionally graded plates under in-plane loads or thermal loads, using an implemented finite element model based on a non-conforming triangular flat plate/shell element associated with a higher order shear deformation theory, is analised in this work. Eigenvalue solutions for linear buckling, and geometrically nonlinear analysis are performed for fully simply-supported and clamped plates. For linear buckling analysis, the results obtained using the present model are in good agreement with the results obtained with alternative models. Furthermore, the predictable occurrence of bifurcation-type buckling described in Tables 14-15 are confirmed by the solutions obtained using the nonlinear analysis.

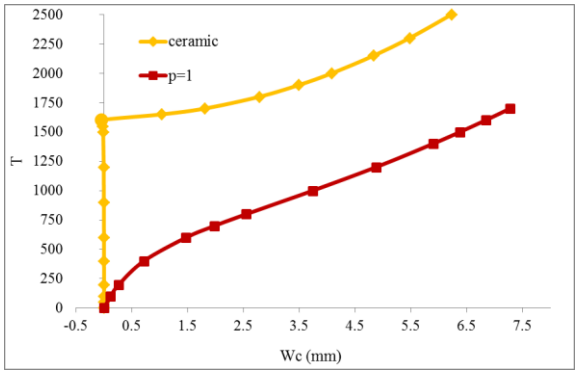

Figure 6. Thermal-displacement path of simply supported plate,under uniform temperature rise.

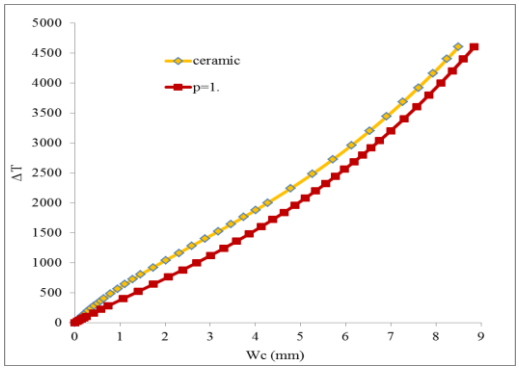

Figure 7. Thermal-displacement path of simply-supported plate under nonlinear temperature distribution.

ACKNOWLEDGEMENTS

This work was supported by FCT, Fundação para a Ciência e Tecnologia, through IDMEC, under LAETA, project UID/EMS/50022/2013, and also CNPq, CAPES and FAPERJ, from Brazil.

REFERENCES

Chakrabarti, A. and Sheikh, A.H., 2003. "Buckling of laminated composite plates by a new element based on higher order shear deformation theory". *Mechanics of Advanced Materials and Structures*, 10 (4), p. 303-317.

Chen, W.J., Lin F.D. and Chen, L.W.,1991."Thermal buckling behavior of thick composite laminated under nonuniform temperature distribution". *Computers & Structures*, 41(4), p. 637-645.

Javaheri, R. and Eslami, M.R., 2002. "Thermal buckling of functionally graded plates based on higher order theory". *Journal of Thermal Stresses*, 25, p. 603–625.

Kozma, F. and Ochoa, O.O., 1986. "Buckling of composite plates using shear deformable finite elements". *AIAA Journal*, 24(10), p. 1721-1724.

Lanhe, W., 2004. "Thermal buckling of a simply supported moderately thick rectangular FGM plate". *Composite Structures*, 64, p. 211–218.

Leissa, A.W., 1986. "Conditions for laminated plates to remain flat under inplane loading". *Composite Structures*, 261-270.

Moita, J.S., Mota Soares, C.M. and Mota Soares, C.A., 1999. "Buckling and dynamic behaviour of laminated composite structures using a discrete higher-order displacement model". *Computers and Structures*, 73, p. 407-423.

Moita, J.S., Barbosa, J.I., Mota Soares, C.M. and Mota Soares, C.A., 2000. "Sensitivity analysis and optimal design of geometric nonlinear laminated plates and shells". *Computers and Structures*, 76, p. 407-420.

Moita, J.S., Araújo, A.L., Mota Soares, CM., Mota Soares, C.A. and Herskovits, J., 2016. "Material and geometric nonlinear analysis of functionally graded plate-shell type structures". *Applied Composite Materials*, 23(4), p. 537–554.

Moita, J.S., Araújo, A.L., Martins, P.G., Mota Soares, C.M. and Mota Soares, C.A., 2011.**"**Analysis of active-passive plate structures using a simple and efficient finite element model". *Mechanics of Advanced Mater. and Struct.*,18, p. 159-169.

Na, K.S. and Kim, J.H., 2006. "Thermal postbuckling investigations of functionally graded plates using 3-D finite element method". *Finite Elements in Analysis and Design*, 42, p. 749 – 756.

Natarajan, S., Ferreira, A.J.M., Bordas, S., Carrera, E., Cinefra, M. and Zenkour, A.M., 2014. "Analysis of functionally graded material plates using triangular elements with cell-based smoothed discrete shear gap method". *Math. Problems in Engineering*, Article ID 247932, p. 1-13.

Nguyen-Xuan, H., Tran, L.V., Thai, C.H. and Nguyen-Thoi, T., 2012. " Analysis of functionally graded plates by an efficient finite element method with node-based strain smoothing". *Thin-Walled Structures*, 54, p. 1-18.

Phan, N.D. and Reddy, J.N., 1985. "Analysis of laminated composite plates using a higher-order shear deformation theory". *Intern. Journal for Numerical Methods in Engineering*, 21, p. 2201-2219.

Qatu, M.S. and Leissa, A.W., 1993. "Buckling or transverse deflections of unsymmetrically laminated plates subjected to in-plane loads". *AIAA Journal*, 31(1), p. 189-194.

Sun, L.X. and Hsu T.R., 1990. "Thermal buckling of laminated composite plates with transverse shear deformation". *Computers & Structures*, 36(5), p. 883-889.

Thai, H.T. and Choi D.H., 2012. "An efficient and simple refined theory for buckling analysis of functionally graded plates". *Applied Mathematical Modelling*, 36, p. 1008–1022.

Thangaratnam, K.R., Palaninatham and Ramachandran J., 1989. "Thermal buckling of composite laminated plates". *Computers and Structures*, 32(5), p. 1117-1124.

Wu, T.S, Shukla, K.K. and Huang, J.H., 2007. "Post-buckling analysis of functionally graded rectangular plates". *Composite Struct.*, 81, p. 1-10.

Zhao, X., Lee, Y.Y. and Liew, K.M., 2009. "Mechanical and thermal buckling analysis of functionally graded plates". *Composite Structures*, 90, p. 161–171.

Zienkiewicz, O.C., 1977. *The Finite Element Method*, New York, USA: McGraw-Hill.

RESPONSIBILITY NOTICE

The authors are the only responsible for the printed material included in this paper.